Available online at www.sciencedirect.com
ScienceDirect
International Journal of Multiphase Flow 34 (2008) 1031–1047
International Journal of Multiphase Flow
www.elsevier.com/locate/ijmulflow

Gas–liquid two phase flow measurement method based on combination instrument of turbine flowmeter and conductance sensor

Gui-Bo Zheng [a], Ning-De Jin [a,*], Xiao-Hui Jia [a], Peng-Ju Lv [b], Xing-Bin Liu [b]

[a] School of Electrical Engineering and Automation, Tianjin University, Tianjin 300072, China
[b] Logging and Testing Services Company, Daqing Oilfield Company, Ltd., Daqing, Heilongjiang 163412, China

Received 3 December 2007; received in revised form 7 March 2008
Available online 3 June 2008

Abstract

In order to solve the flowrate measurement problem of gas–liquid two phase flow widely existing in gas wells of Daqing oil field in China, a new method has been developed, which is based on the combination instrument of turbine flowmeter and conductance sensor with petal type concentrating flow diverter. The turbine and conductance signals under 104 different flow conditions have been acquired through oil–gas–water three phase flow loop experimental facility. To determine the flow pattern in measurement channel, attractor morphologic characteristics are extracted from the conductance signals. For the total flowrate measurement, based on the turbine fluctuant signals of gas–liquid two phase flow, a statistical model with the average error of 7.9% is set up. With regard to the water cut measurement, the characteristics in time and frequency domains are extracted from the fluctuant conductance signals, and then employing the Support Vector Machine (SVM) soft measurement model used in high-dimension data fitting, the water cut prediction is realized with the average error of 0.038. The results show that the combination instrument of turbine flowmeter and conductance sensor with petal type concentrating flow diverter would be useful in measuring the total flowrate and water cut of gas–liquid two phase flow in gas production wells.

Keywords: Gas–liquid two phase flow; Turbine flowmeter; Conductance sensor; Flow pattern characteristics; Water cut; Soft measurement technique

1. Introduction

Gas–liquid two phase flow is a common flow phenomena existing in petroleum industry, chemical engineering and other related process production, the flow measurement is a basic problem in these fields. Because the flow structure and distribution of phase interfaces change with time and space, the gas–water two phase flow measurement is much more difficult than that of single phase flow, which remains unsolved thoroughly. Recently, with the increasing of gas production wells exploited in Daqing oil field of China, searching for an effective method to measure the flowrate of gas–liquid two phase flow has become more and more important.

In early studies, Jones (1983), Mendes and Marvillet (1996) and Oddie and Pearson (2004) had made detailed review in the gas–liquid two phase flow measurement techniques. Because of the complicated and variable characteristics of gas–liquid two phase flow patterns, single sensor cannot implement the precise flowrate measurement, however the combination of two or more kinds of sensors makes precise flowrate measurement possible (Abdul-Razzak et al., 1995a,b; Frank et al., 1977; Huang et al., 2005; Shim and Lee, 1998; Shim et al., 1996). Among the combination methods, the one based on combination instrument of single phase flowmeter with densimeter or void fraction meter come to be one of the main trends of current two phase flow measurement because of its simple structure and easy realization.

* Corresponding author. Tel./fax: +86 22 27407641.
E-mail address: ndjin@tju.edu.cn (N.-D. Jin).

0301-9322/$ - see front matter © 2008 Elsevier Ltd. All rights reserved.
doi:10.1016/j.ijmultiphaseflow.2008.05.002

In recent years, much progress had been achieved by employing turbine flowmeter to measure multiphase flowrate. Mark et al. (1990) provided a measurement of the liquid flowrate by analyzing the pulse output information from a standard turbine meter in gas–liquid two phase flows whose void fraction is up to 20%, and they also pointed out that the single phase performance remained unaffected when using turbine flowmeter measure two phase flow. Johnson and Farroll (1995) put forward a technique to determine the void fraction of vertical upward gas–water two phase flows by measuring the turbine meter signal, the test results showed that the measuring precision could be ± 0.02 when the void fraction was below 10%. Abdul-Razzak et al. (1995a) had used the combination of turbine flowmeter and void fraction meter to measure the mass flowrate of refrigerant liquid–vapor two phase flow, they also researched different prediction model of mass flowrate, and pointed out that the volumetric homogeneous model showed better performance at high flowrate. Abdul-Razzak et al. (1995b) had also used the combination of turbine flowmeter and Venturi flowmeter to measure the mass flowrate of refrigerant liquid–vapor two phase flow and pointed out this combination was superior to the combination of voidage meter with either turbine flowmeter or Venturi flowmeter. Minemura et al. (1996) proved the feasibility of measuring the mass flowrate, volume flowrate and void fraction of gas–liquid two phase flow accurately using the turbine flowmeter through experiments, and they also indicated that the mass flowrate and volume flowrate could be expressed as the function of rotor speed and pressure drop across turbine flowmeter. Shim and Lee (1998) suggested a method to measure the flowrate of individual phase by setting turbine flowmeter and Gamma densimeter at upstream and downstream separately of the vertical upward pipe, they also showed that the output signals of turbine flowmeter only depended on the volume flowrate of gas and liquid. Ogawa et al. (1998) designed a new flowrate measurement system based on the former research results of two phase flow measurement using turbine flowmeter, and finally an instrument to measure the flowrate of oil–gas–water three phase flows was carried out through tests of air–high viscous liquid mixtures.

The determination of the void fraction of two phase flow has great significance to the optimization of industry process and flow control. Because of the simple structure and the ability to get one-dimensional continuous signals related to the fraction of fluid, the impedance method has been widely used in this field. Hardy and Hylton (1984) determined the void fraction and flow velocity by using string impedance probes to simultaneously measure the conductance and capacitance signals of two phase flow, the string probe instrumentation proved to be capable in measurement of either air–water or steam–water flows and demonstrated an ability to measure a wide range of flow velocities and void fractions. Ma et al. (1990) had pointed out that impedance method is an effective way to measure the void fraction and they established a theoretical measurement model of phase fraction based on impedance signals, and the test results showed that most of the measured void fractions are within a $\pm 10\%$ errors band as compared with the actual void fraction. Lucas et al. (2000) designed and constructed a local six-electrode conductivity probe to simultaneously measure the local solids volume fraction and the local solids axial velocity with high precision in solids-water pipe flows. To investigate the relationship between void fraction and volume-averaged impedance in air–water mixtures, Yang et al. (2003) had used styrofoam spheres, whose relative permittivity was negligible compared to that of water to simulate the gas bubble, they got the measurement result whose deviation maintained within 0.5% when the void fraction range is from 0 to 0.1.

With the developing of modern signal processing techniques, there has been much progress in flow parameters measuring methods based on the soft measurement techniques (Jin et al., 2006; Peng and Mi, 2006; Peng and Liu, 2006). The Support Vector Machine (SVM) (Vapnik, 1995; Vapnik, 1999) is a newly developed soft measurement method based on the statistical learning; it could make highly precise estimation to measured data without any specific model. Also, because the SVM does not have the local minimization problem and its computational complexity has no relation with the dimension of input samples, it has been gradually applied to the estimation of phase fraction in multiphase flow (Jin et al., 2006; Peng and Mi, 2006).

Although there has been some achievement in the measurement of two phase flow using the turbine flowmeter and impedance sensors, the measurement precision cannot be guaranteed except under low gas fraction conditions, furthermore, the measurement results are still greatly influenced by the flow patterns. There also exist many difficulties in establishing a precise prediction model for volume fraction measurement, so it is significant to study on the soft measurement method to measure volume fraction and flowrate of gas–liquid two phase flow. In this study, we have used the combination instrument of turbine flowmeter and conductance sensors with petal type concentrating flow diverter to acquire the fluctuant conductance signals in the concentrating flow measurement channel, which can improve the uniformity of gas–liquid two phase flow and be useful for the total flowrate measurement. We also have, respectively, used two kinds of methods to determine the flow pattern, one is the traditional statistical signal analysis, and the other is the chaotic attractor morphologic description method of nonlinear time series. Then we extracted several characteristics in time and frequency domains to fulfill the estimation of water cut by applying them to SVM. Combined with the measurement results of total flowrate gotten from turbine flowmeter, the final results show that the combination instrument of turbine flowmeter and conductance sensor with petal type concentrating flow diverter could be useful in measuring the total flowrate and the water cut of gas–liquid two phase flow in gas production wells.

2. The experimental flow loop facility and data acquisition

The gas–water two phase flow experiments in vertical upward pipe were carried out in oil–gas–water three phase flow laboratory of Tianjin University, the related measuring instruments are shown in Fig. 1. The instrument is composed circuit tube, conductance sensors, a turbine flowmeter and a petal type concentrating flow diverter. The diverter is mainly composed of switching circuit, concentrating petal, pushing and pulling mechanism, power-off switch, adjusting mechanism and micromotor. The working process is like this, when the switching circuit provides working voltage to the micromotor, the micromotor enables the pushing and pulling mechanism, which makes the petal open or close, when the petal opens to a certain position, the power-off switch turns-off the switching circuit. The adjusting mechanism aims to adjust the open degree of the petal. The petal is constructed by reinforcement and nylon cloth, when the petal opens fully, the ring borders of it clings to the inner wall of the pipe, forcing the fluid flow into the concentrating channel through the petal type diverter.

The experimental flow loop facility is shown as Fig. 2, it mainly include three parts, which are separately the oil/gas/water three channels supply system, the simulation oil pipe and the control system. The flowrate of the oil, gas, water can be controlled by the opening of valve through the control system, in order to get the different flowrate and water cut. The flowrate of gas and water phase are, respectively, measured by Vortex flowmeter and Roots flowmeter, the results from which are also recorded and displayed by the computer of the control system. The height of the simulation well pipe is 6 m, including two Plexiglas pipes with inner diameter of 125 and 80 mm, respectively, they could be controlled to incline within the scope of 0–90 deg. There is a quick closing valve on the well pipe whose inner diameter is 125 mm, which is used to measure the water holdup of two phases mixed fluid. The instruments used in this research are all in the oil industrial standard size, the detailed structure is shown in Fig. 1, the outer diameter of the instrument is 23 mm, inner diameter is 18 mm. The whole measurement system can be divided into several parts, which are turbine flowmeter, conductance sensors, exciting signals generating circuit, respectively, signal modulating module, data acquisition device and signal analysis software. The measurement circuit is embedded inside the instrument, and signals were transmitted to the data acquisition and processing system through cable connected outside the circuit tube. Through the concentrating diverter, the fluid flow into the measurement channel, then passing the turbine flow meter and the conductance sensors, the fluid flow out from the liquid holes at the upper place of the instrument. The measurement system uses the 20 kHz constant voltage sine wave to excite, and the virtual value of exciting voltage is 1.4 V. The signal modulating module is mainly constitutes by three modules, which are differential amplifier, sensitive demodulation and low pass filter. The data acquisition equipment is selected from the National Instrument Company's product PXI 4472 data acquisition card, which is based on the PXI main bus technology, equipped with eight channels and synchronized acquiring function. The data processing part is realized through graphical programming language LABVIEW 7.1 wrapped in the data acquisition card, which can realize real time data waveform displaying, storing and analyzing.

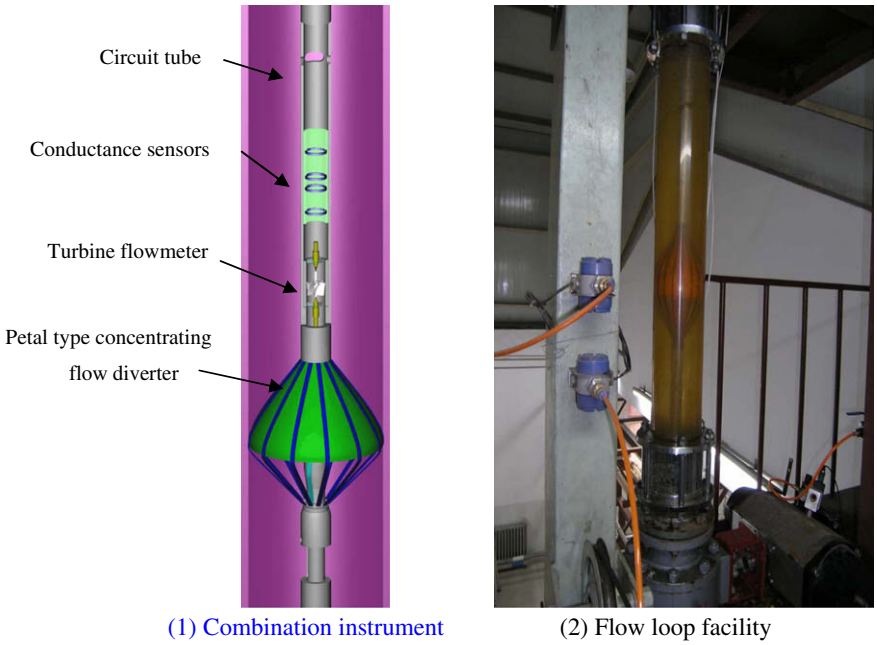

(1) Combination instrument (2) Flow loop facility

Fig. 1. Combination instrument and experimental flow loop facility.

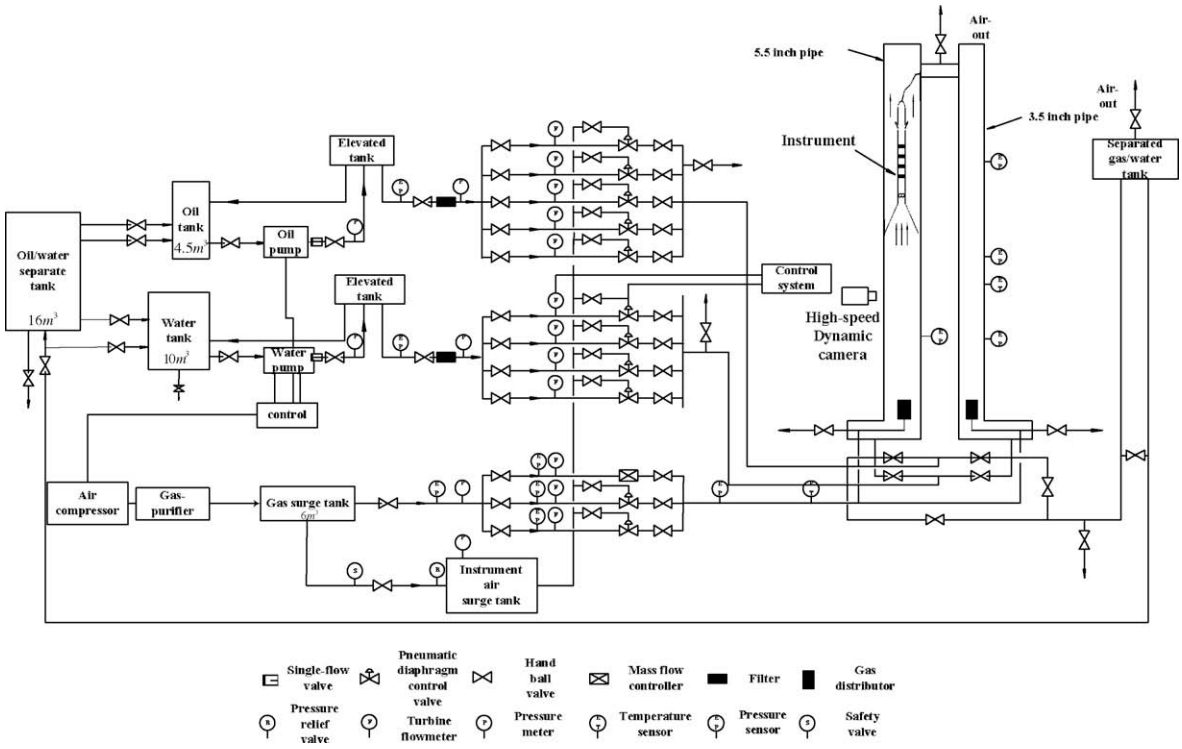

Fig. 2. Configuration of experimental flow loop facility.

The experimental mediums are air and tap water. The water at certain flowrate is injected into pipe firstly when we do the experiments, and then the gas flowrate Q_g is gradually increased. After completing configuring the ratio of gas and water phase each time, we observe and record the flow patterns of gas–liquid two phase flows. The total flowrate Q_t of gas–water two phase flow ranges from 0.1 to 2.5 m^3/h in the experiments. The sampling frequency of conductance signal is 400 Hz; sampling time is 60 s at each test point. The sampling frequency of turbine flowmeter is 1 Hz, sampling time is 100 s, and the resultant sample size is 100 data points at each flow condition. The sampling frequency and sampling time are very sensitive to the measurement; there had been serious consideration for this when choosing them. Based on the existing experiment data and references related to this, the inherent frequency of gas–liquid two phase flow will not exceed 50 Hz; from the Shannon theory the sampled signal can be recurred as long as the sampling frequency is twice more than the inherent frequency of the sampled parameter. Also, as the Fig. 8 showing, the inherent frequency of gas–liquid two phase flow is just distributed within 40 Hz, so the sampling frequency 400 Hz in this paper is reasonable, which could not only recur the signal fully, but also attain high precision. When setting up the prediction model for total flowrate and water cut, the average value of the turbine signal is only used, therefore the sampling frequency does not need to be very high. The sampling frequency of 1 Hz is selected, but even this frequency could still reflect the change of the total flowrate. Measurement signals under 104 gas–water two phase flow conditions have been acquired in the experiment all together.

Fig. 3 shows the motion process of bubble flow recorded by high speed VCR (Video Camera Recorder), the numbers and the arrows indicate the motion direction. When the air fraction is low, air phase is the dissipation phase and the water phase is continuous phase. The air dissipates in flowing upward fluid at the form of different size bubble randomly, and the phase interface is clear. The bubbles appear various shape, most of them present flat sphere of different size, the bubble size increases with the increasing of air fraction. In total, the bubble flow has uniform flow structure. Fig. 4 shows the motion process of slug flow recorded by high speed VCR. When the concentration of bubbles in the bubble flow increase, bubbles begin to aggregate. As the diameter of bubble growing, close to the inner diameter of the pipe, it evolves into a projectile bubble. While the big projectile type bubble passes through, the small bubbles around are forced to fall down, the phase interface is comparatively clear at this time; once the bubbles meet the following liquid slug, there comes collision, then the small bubbles amalgamate into the liquid group, and flow upward, the interface becomes blur at this moment, and the flow condition is complicated. As the flowrate of gas increases, the length of projectile type gas bubble grows.

Figs. 5 and 6 show the turbine and conductance fluctuant signals of typical flow conditions sampled by measuring instrument, and the flow patterns marked in figures were that observed by eyes. Because the flow patterns cannot

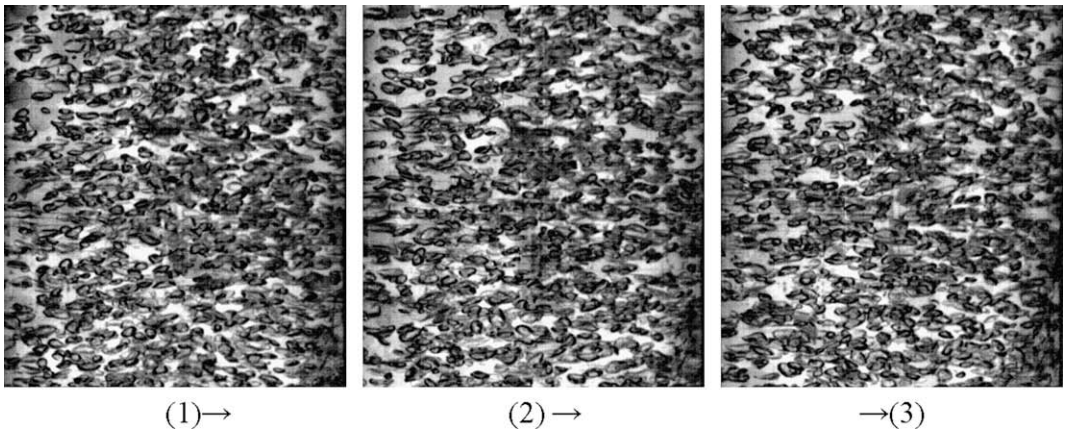

Fig. 3. Motion process of bubble flow.

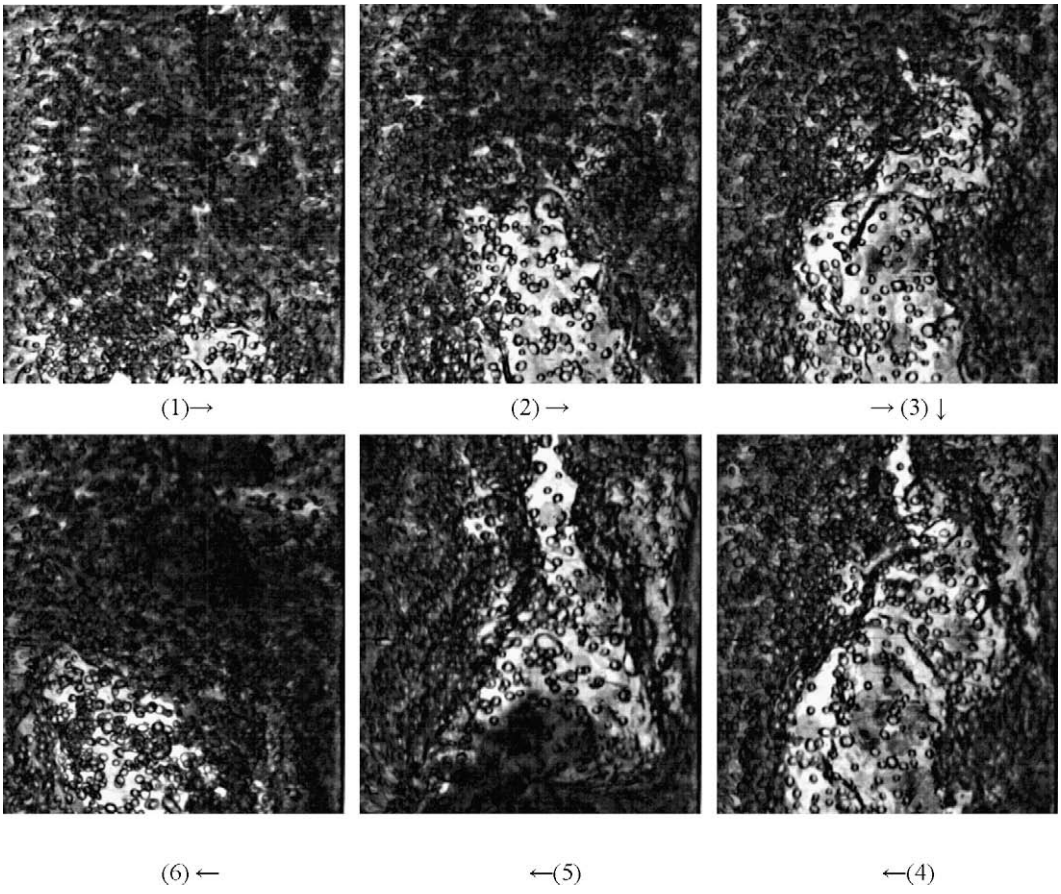

Fig. 4. Motion process of slug flow.

be recognized visually and there is no principle for flow pattern classification of flow in concentrating flow channel also, the flow pattern classification in concentrating flow channel can only be carried out by observing the flow patterns before the flow enters into the concentrating flow channel and refer to the classification criterion of non-concentrated flow. From Figs. 5 and 6, the similar fluctuant features can be seen from the turbine and conductance fluctuant signals at same flow condition. The curves of top three flow conditions show stochastic, small amplitude oscillation, which is just the feature of random motion of bubble groups dispersed in water. The big amplitude fluctuation occurs on the curves of three flow conditions below, coincident with the character of slug flow, in which air slug and liquid slug appear intermittently and alternately. The flow patterns characteristics gotten from the fluctuant signals are consistent with that observed before the flow enter into the diverter channel, it provides a

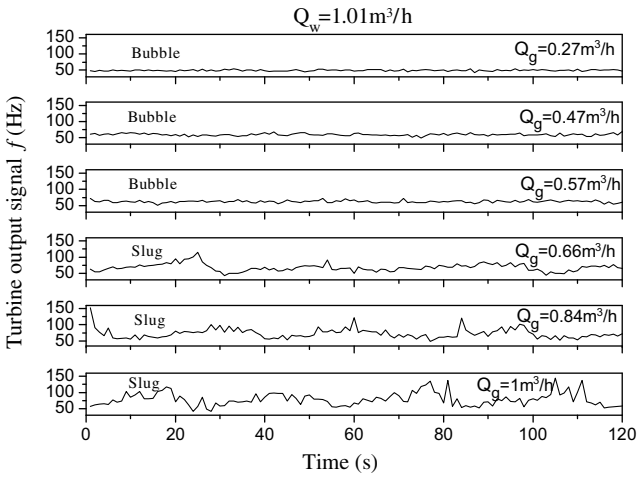

Fig. 5. Turbine fluctuant signals in gas–water two phase flow.

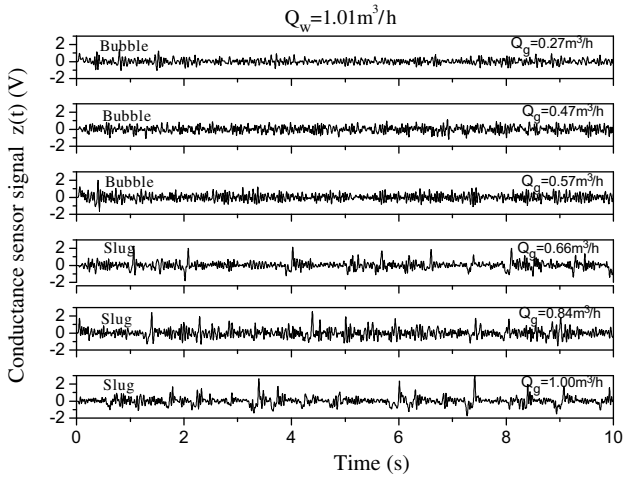

Fig. 6. Conductance fluctuant signals in gas–water two phase flow.

reference for the flow pattern classification using nonlinear method in the following discussion.

3. The conductance sensor signal statistical analysis

The research on statistical flow patterns classification has been carried out for many years based on engineering measurable stochastic signals. Jones and Zuber (1975), Vince and Lahey (1982), Matsui (1984), Kelessidis and Dukler (1989) had all studied the flow pattern classification using probability density function and power spectral density of engineering signals, by analyzing the distribution profiles of these, they had gotten satisfied classification results.

Probability density function (PDF) can manifest the characteristics of the original fluctuant signals and is defined as Eq. (1), which means that the signal is divided into certain intervals equally; the probability P_i is expressed as the ratio of number of signal amplitude in each interval and the sample size.

$$P_i = \frac{n_i}{N} \tag{1}$$

where P_i is probability density, n_i is the number of signal amplitude in each interval, N is the sample size.

In order to verify the validity of PDF for flow pattern classification of flow in concentrating flow channel, PDF distribution of 6 flow conditions at different gas flowrate are shown as Fig. 7, of which the liquid flowrate is 1.01 m^3/h. From the results of PDF, we can see that all the peak values under different flow conditions are distributed between −1.0 and 1.0, furthermore, the peak value of PDF under slug flow conditions is obviously higher than that under bubble flow conditions.

Power spectral density (PSD) can reflect the distribution of original signals at different frequency band through the investigation of statistical characteristics in frequency domain after Fourier transformation, and the discrete equation is shown as follow:

$$S_Z(w) = \frac{1}{N}\sum_{n=0}^{N-1} R_Z(\tau)e^{-jwn} \tag{2}$$

where $R_Z(\tau)$ is the auto correlation function of discrete signal $Z(t)$, it is defined as follow:

$$R_Z(\tau) = \lim_{T\to\infty}\frac{1}{T}\int_0^T z(t+\tau)z(t)\,dt \tag{3}$$

Fig. 8 is the power spectral density of the flow under conditions of which gas flowrate changes with the liquid flowrate maintains at 1.01 m^3/h. As the figure shown, the power of all the flow conditions disperse from 0 to 35 Hz, and increase with the increasing of gas flowrate, but there is no obvious boundary can be seen form the power peak of different flow patterns, and the location of the power peak is random relatively. No obvious characteristics can be found to identify the bubble flow and slug flow from the PSD.

From the analysis of PDF and PSD above, the results of flow pattern classification are not satisfactory as expected. Although amplitude of PDF can roughly classify the flow patterns, the selection of criterion is subjective in some sense, which is not favorable for the correct classification of flow patterns. It is necessary to find new methods to fulfill the quick and correct classification of flow patterns.

4. The chaotic attractor morphologic analysis of conductance signal

In early study, Franca et al. (1991) proposed the nonlinear time series analysis for the flow pattern classification. Using nonlinear dynamic method to analyze the characteristics of two phase flow measurement fluctuant signals could be useful exploration for revealing and understanding the flow pattern transmission mechanism which cannot be described accurately by mathematical model because of the complexity and uncertainty it owns. Recently, Annunziato and Abarbanel (1999) put forward attractor morpho-

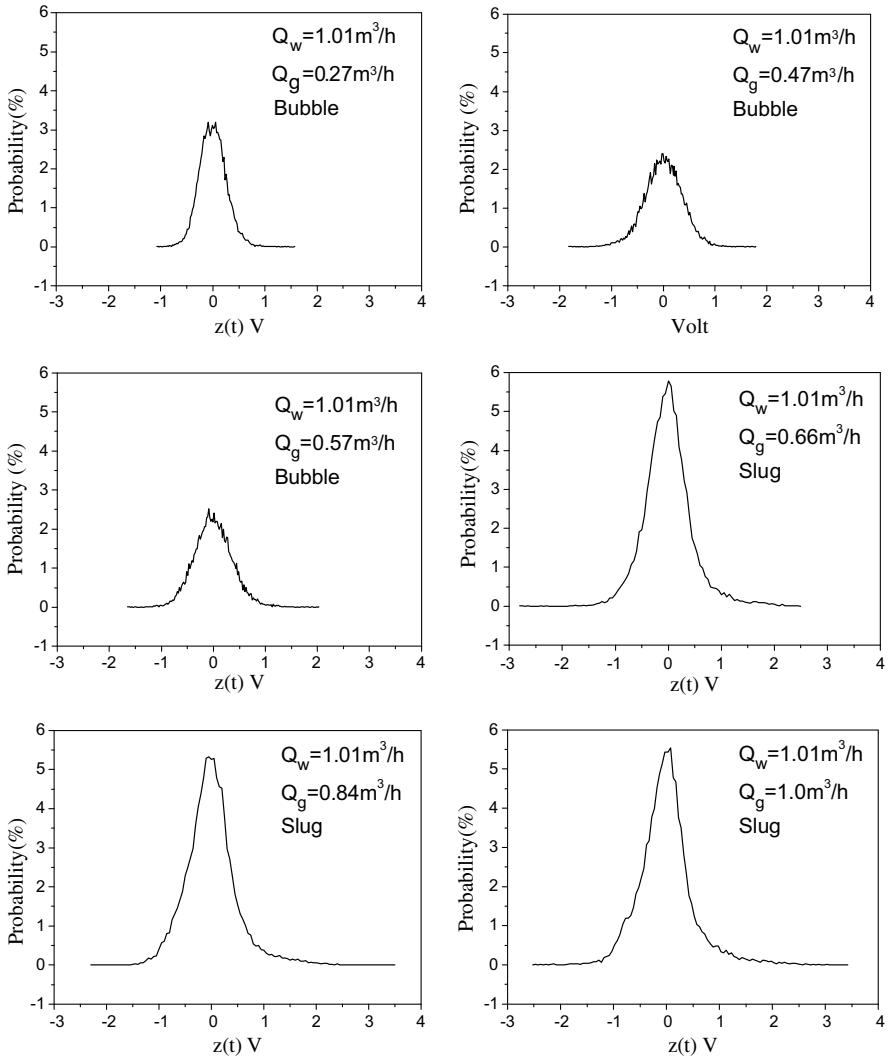

Fig. 7. PDF distribution of different gas flowrate conditions at $Q_w = 1.01$ m^3/h.

logic description method, and applied it to flow pattern classification. The research results indicate that the method possesses quick computation characteristic and can get good results of the flow patterns classification. Llauro and Llop (2006) analyzed the flow patterns of gas–solid two phase flow using this method and got good classification results too. Xiao and Jin (2007) employed the method to study the pressure fluctuant signals of gas–liquid two phase flow in vertical upward pipe, and realized the effective classification of flow patterns.

4.1. The attractor moments

In order to study the attractor shape, the original signal should be taken phase space reconstruction based on Takens's embedding theorem (Takens, 1981) at selected certain delay time and embedding dimension. Takens's embedding theorem can be described as following, for arbitrary time series $z(it)$, $i = 1, 2 \ldots, n$ (t is sampling interval, n is the sample size), if the embedding delay time is selected as τ, and the embedding dimension as K, the vector point in phase space can be represented as follow:

$$\begin{aligned}\vec{\mathbf{X}}(k) &= \{x_1(k), x_2(k), \ldots, x_N(k)\} \\ &= \{z(kt), z(kt+\tau), \ldots, z(kt+(K-1)\tau)\}\end{aligned} \tag{4}$$

where $k = 1, 2, \ldots, M$, $M = n - (K-1)^* \tau/t$ denotes the total points of attractor after phase space reconstruction.

The shape and structure of chaotic attractor in phase space is the important base of determining the movement states of nonlinear system. Studying the attractor shape in two-dimension spaces, we only need to care about two coordinates $X_i = z(it)$, $Y_i = z(it+\tau)$, where $z(it)$ is the observed time series, t is sampling interval and τ is the delay time increasing from zero.

Figs. 9 and 10 show the evolving of the two-dimension attractor with increasing delay time τ of typical bubble and slug flow conditions, respectively. It can be seen from the figures that two-dimension attractor are compressed near the first and third quadrants when τ is very small and unfold gradually with the increasing of τ, but when τ

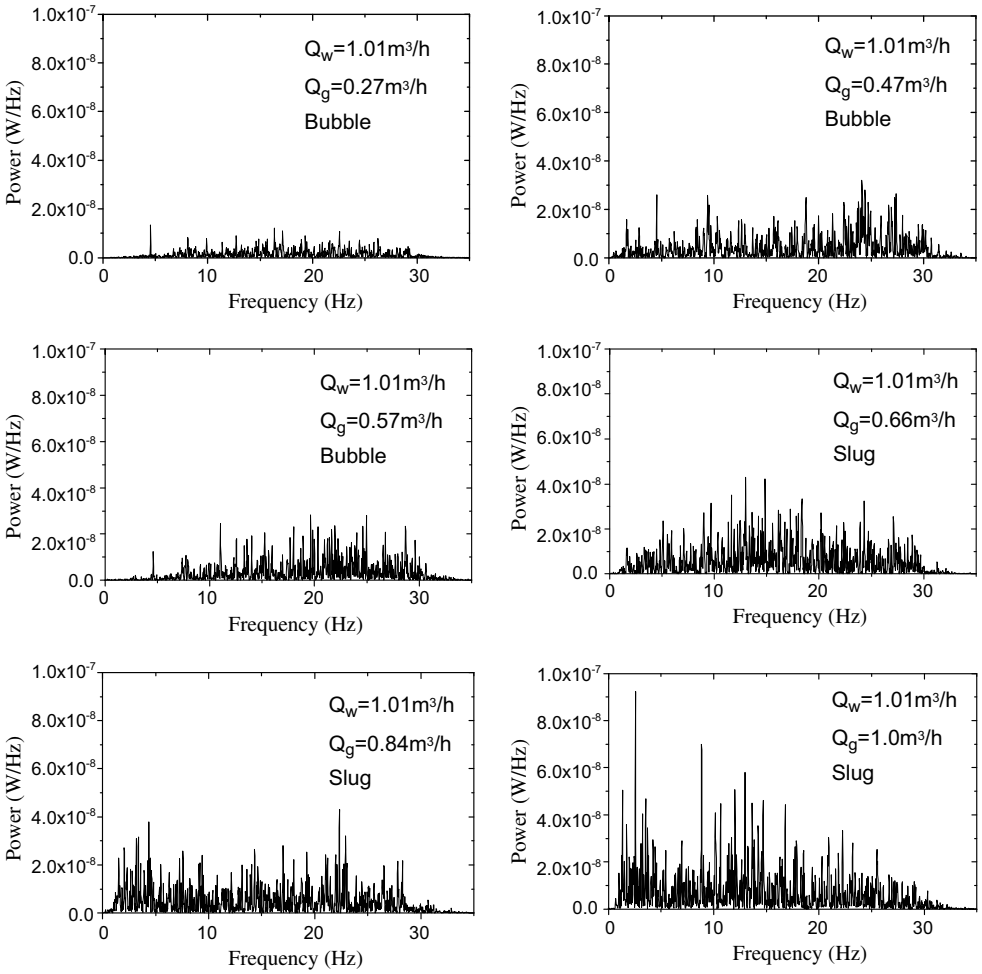

Fig. 8. PSD distribution of different gas flowrate conditions at $Q_w = 1.01\ m^3/h$.

increases to certain value (12.5–17.5 ms) the attractor shape begin to reverse suddenly and lose the topological shape in unfolding process. The trend can also be seen that the decentralization degree to the bisector of first and third quadrants increases with the increasing of τ, while that to the second and fourth quadrants decreases with the increasing of τ. Annunziato and Abarbanel (1999) pointed out the morphological differences of the different flow patterns are evident, but the description of the attractor shape is quite difficult because it depend strongly by the time lag. Because of the difficulty existing in the description of attractor morphology and the subjectivity in classifying the flow patterns, there has proposed attractor morphologic characteristics method in this study, which is more objective.

In this study, the methods proposed by Annunziato and Abarbanel (1999) and Llauro and Llop (2006) are used, which mainly involves selecting bisector of first and third quadrants (called principal axis), bisector of second and fourth quadrants (called secondary axis) and original point to study the symmetry of attractors. The distances of each point on attractor to the two axes and original point can be defined as followed:

$$d_{1,i} = \frac{\sqrt{2}}{2}(X_i - Y_i) \tag{5}$$

$$d_{2,i} = \frac{\sqrt{2}}{2}(X_i + Y_i) \tag{6}$$

$$d_{3,i} = \sqrt{X_i^2 + Y_i^2} \tag{7}$$

with every distance it is possible to define some moments with order j as follow:

$$M_{m,j}(\tau) = \frac{\sum_{i=1}^{N} d_{m,j}^{j}}{N} \tag{8}$$

where N is the number of samples and $m = 1, 2, 3$ denotes the kind of distance considered.

Starting from $\tau = 0$, the attractor is compressed on the principal axis when τ increases, these moments describe the morphological evolution during the unfolding process of the attractor. The moments evolve from the linear value (for $\tau = 0$) to nonlinear one. Finally we can outline that the even moments are always positive and describe the scatter of the attractor, while the odd moments are symmetry descriptors.

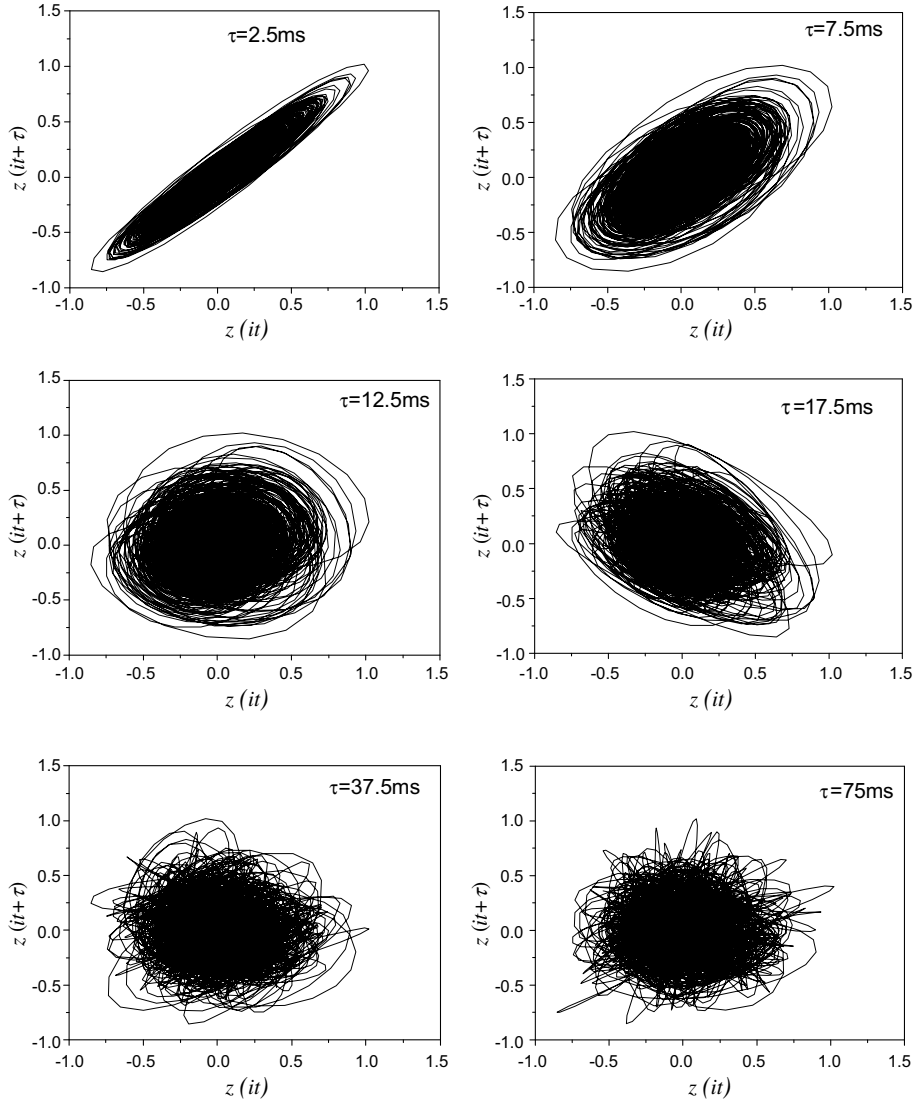

Fig. 9. Typical attractor shape of bubble flow at different delay time ($Q_w = 1.01\ m^3/h$, $Q_g = 0.27\ m^3/h$).

4.2. The extraction of attractor morphologic characteristics

The attractor corresponding to increasing delay time τ from zero is called dynamic attractor. Combining with attractor moments, the curve $M_{i,j}(\tau) \sim \tau$ of attractor moments of dynamic attractor changing with delay time τ can be figured out. Further, the influence of the selection of delay time can be weakened by defining new variables.

After certain time delaying if the curve $M_{i,j}(\tau) \sim \tau$ appears maximum or minimum, then the corresponding delay time is defined as transform delay time τ_f. If there is no extremum, the delay time corresponding to suddenly changing of slope of the curve can also be called as the transform delay time τ_f. The part before τ_f is called first area and the part after τ_f is called second area.

The first area represents the unfolding process of attractor from the compressed state at small delay time to topology structure at suitable delay time. This area is approximately linear, so the slope of the area can serve as characteristic, namely, attractor morphologic characteristics, denoted as $SM_{i,j}$, and the following equation should be satisfied.

$$M_{i,j}(\tau) \approx \mathrm{SM}_{i,j} \cdot \tau + \mathrm{IM}_{i,j} \quad (0 \leqslant \tau \leqslant \tau_f) \tag{9}$$

where $IM_{i,j}$ is the intercept of curve. In interval of $0 \leqslant \tau \leqslant \tau_f$ fitting the attractor moments and delay time τ using minimal least square method, the approximately slope of curve in first area, i.e. attractor morphologic characteristic, can be gotten. Obviously, the attractor morphologic characteristic has no certain relation with the value of delay time, so the error brought by the improper selection of delay time can be weakened.

The second area after τ_f reflects the irregular state when attractor structure comes to reverse, so the curve $M_{i,j}(\tau) \sim \tau$ behaves as fluctuating or slope changing suddenly.

The relations between two-dimension attractor moments of $M_{1,2}$, $M_{2,2}$ and embedding delay time are shown in Fig. 11. As the figure shown, the curves

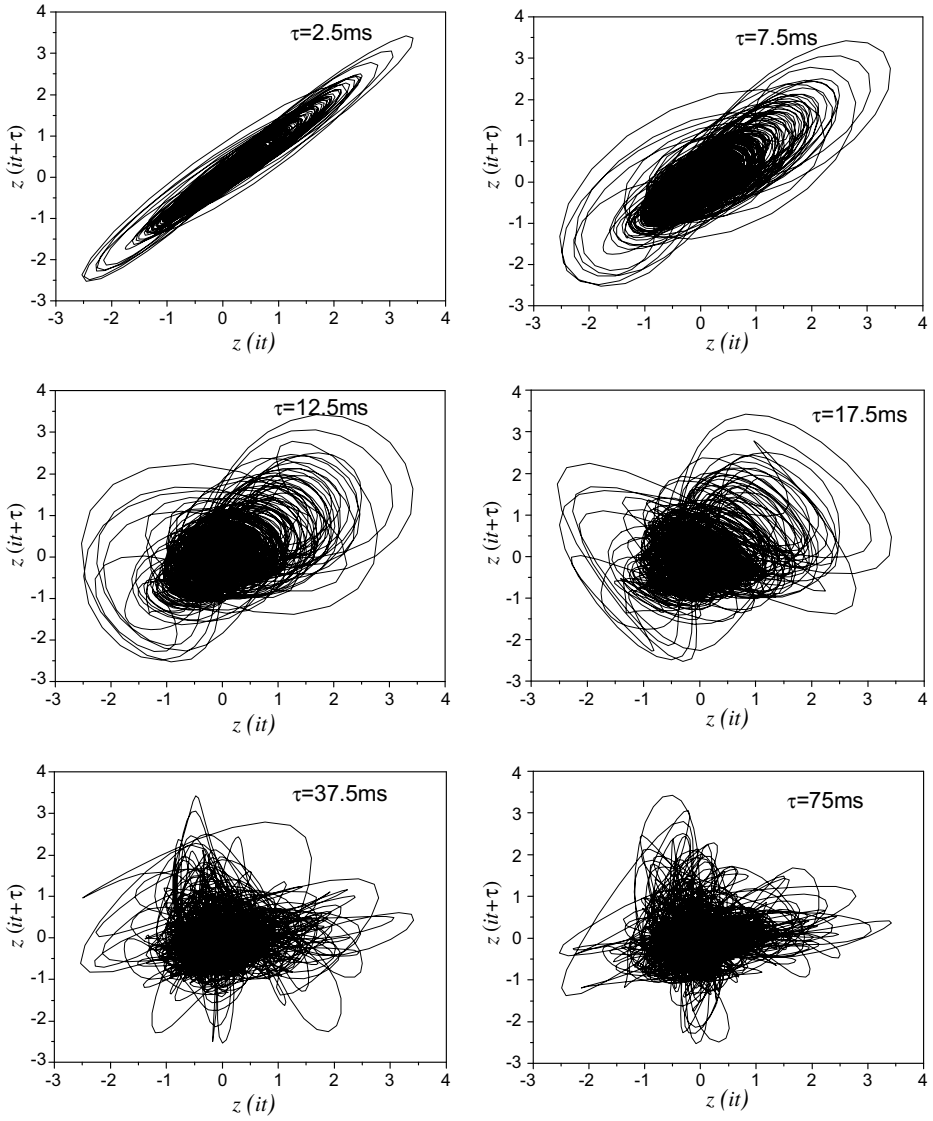

Fig. 10. Typical attractor shape of slug flow at different delay time ($Q_w = 1.01\ m^3/h$, $Q_g = 1.0\ m^3/h$).

$M_{1,2} \sim \tau$ and $M_{2,2} \sim \tau$ could both be found extremum, so the corresponding delay time can be selected as τ_f whose value is about 10 ms. Calculating the slope of curve and getting attractor morphologic characteristics, we can use them to identify the flow patterns.

4.3. The flow pattern classification

In order to classify the flow patterns using attractor morphologic characteristics we have studied the sensitivity and distribution of two-dimensional attractor morphologic

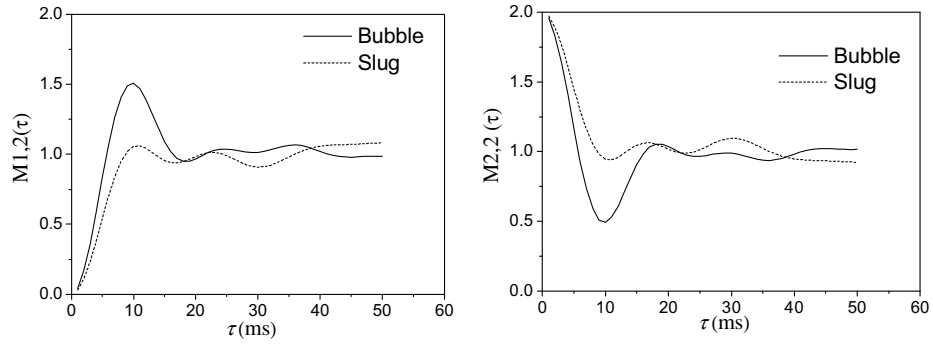

Fig. 11. $M_{1,2}(\tau) \sim \tau$ and $M_{2,2}(\tau) \sim \tau$ curves of different flow patterns.

characteristics of each order of flow patterns under 104 flow conditions and the results are shown as Fig. 12.

As Fig. 12 shown, only $SM_{1,2}$ and $SM_{2,2}$ two characteristics are sensitive to flow patterns and have good classification results for most flow conditions. So these two characteristics are selected as effective characteristics group for flow patterns classification. Fig. 13 show the flow patterns distribution of 104 flow conditions on the plane $SM_{2,2}$–$SM_{1,2}$ constituted with $SM_{1,2}$ and $SM_{2,2}$. As the figure showing, the plane can classify bubble and slug flow patterns and separating point locates at the crossing of the two dot line in the figure.

Observing the figure carefully, we can see that only 4 flow conditions are not identified correctly, of which two bubble flow conditions locate wrongly in slug identification area and two slug flow conditions locate in bubble identification area. The final result is that only 4 of 104 flow conditions get wrong classification and the accuracy is higher than 96%. The research results indicate that the attractor morphologic characteristics are helpful to identify the flow patterns of flow conditions in the experiment, making the flow patterns be classified linearly, which would be useful guidance for the studying of complex gas–liquid two phase flow.

5. The turbine flowmeter model in gas–water two phase flow

The turbine flowmeter is a kind of velocity type flowmeter which is composed of turbine, bearing and the preamplifier. The turbine is pushed to rotate when the flow along the axial line of the pipe impacts the blades of flowmeter. At the same time, the blades cut through the magnetic lines excited by electromagnet periodically, change the magnetic flux of the coils as well. Based on the electromagnetic induction principle, fluctuant electric potential signals will be inducted in the coils, whose frequency is in direct ratio to the flowrate of the measured flow. The constant of the instrument is an important parameter, which shows the number of impulse output by every cubic meter of flow. It is usually calibrated under normal temperature in clean water before being used. The output signals from the turbine transmitter is input into the display instrument after being amplified through the preamplifier, and then the flowrate measurement is fulfilled, and the relationship between the rotate speed of the turbine and the flowrate is showed as follow:

$$f = K(Q_t - Q_0) \tag{10}$$

where Q_t is the total flowrate (m^3/h), Q_0 is the threshold flowrate of the turbine flowmeter (m^3/h), f is the rotating speed of the turbine (Hz), K is the meter factor.

The research object is the fluid in the concentrating channel, as the diameter of flow channel after concentrating diverter is very small (inner diameter is 18 mm), the velocity profile of fluid in the concentrating channel tends to be uniform, which can reduce the influences of flow patterns on the measuring characteristics of the turbine flowmeter, making the responses of turbine flowmeter shows reasonable correlation with the total flowrate of gas–liquid two phase flow, which means there would be total flowrate measuring results with acceptable precision.

According to the turbine fluctuant signals and the corresponding flowrate data, we can get the statistical model for total flowrate prediction as Eq. (11) and the results are shown as Fig. 14.

$$Q_{pre} = (-1.07428E-4)f^2 + 0.04128f - 0.55025 \tag{11}$$

The error is calculated with Eqs. (12) and (13) APE is the average percent error, and AE is the average error. T_i is the predicted value, Y_i is the experimental value, N is the size of sample data.

$$APE = \frac{1}{N}\sum_{i=1}^{N}\left|\frac{T_i - Y_i}{T_i}\right| \tag{12}$$

$$AE = \frac{1}{N}\sum_{i=1}^{N}|T_i - Y_i| \tag{13}$$

From the prediction results of total flowrate shown as Fig. 15 based on the statistical model, we can know that the average error is 0.089 m^3/h and the average percent error is 7.9%, which means the statistical model based on the turbine rotating speed data could be a acceptable prediction model for total flowrate.

The turbine flowmeter is mostly used to measure the single phase flow; the flow pattern will affect its measurement precision when used in two phase flow. The total flowrate model is set up without considering the influence of flow patterns, so there should be some error. But for an industrial instrument and measurement, the measuring error of 7.9% is acceptable.

6. The water cut soft measurement technique

The learning method based on SVM has attracted more and more attention in the academic fields, and it also has been widely applied to solve the classification and regression problems in the soft measurement modeling area. The most obvious characteristic of SVM is the structural risk minimization principle it has adopted, which is fit for small training sample, and its strong generalization ability. Besides, SVM has skillfully solved the problems such like complex computation, dimension disaster, local minimization and so on, by using one kernel function to substitute the inner product operation in high-dimension space after turn the nonlinear problem into a linear problem in high-dimension space.

6.1. The characteristics extraction of conductance signal in time and frequency domains

Choosing proper characteristics is the key step using Support Vector Machine (SVM) method to predict water cut, which means the characteristics chosen should reflect features of the original signals as much as possible. In this study, we have extracted 11 indexes from fluctuant

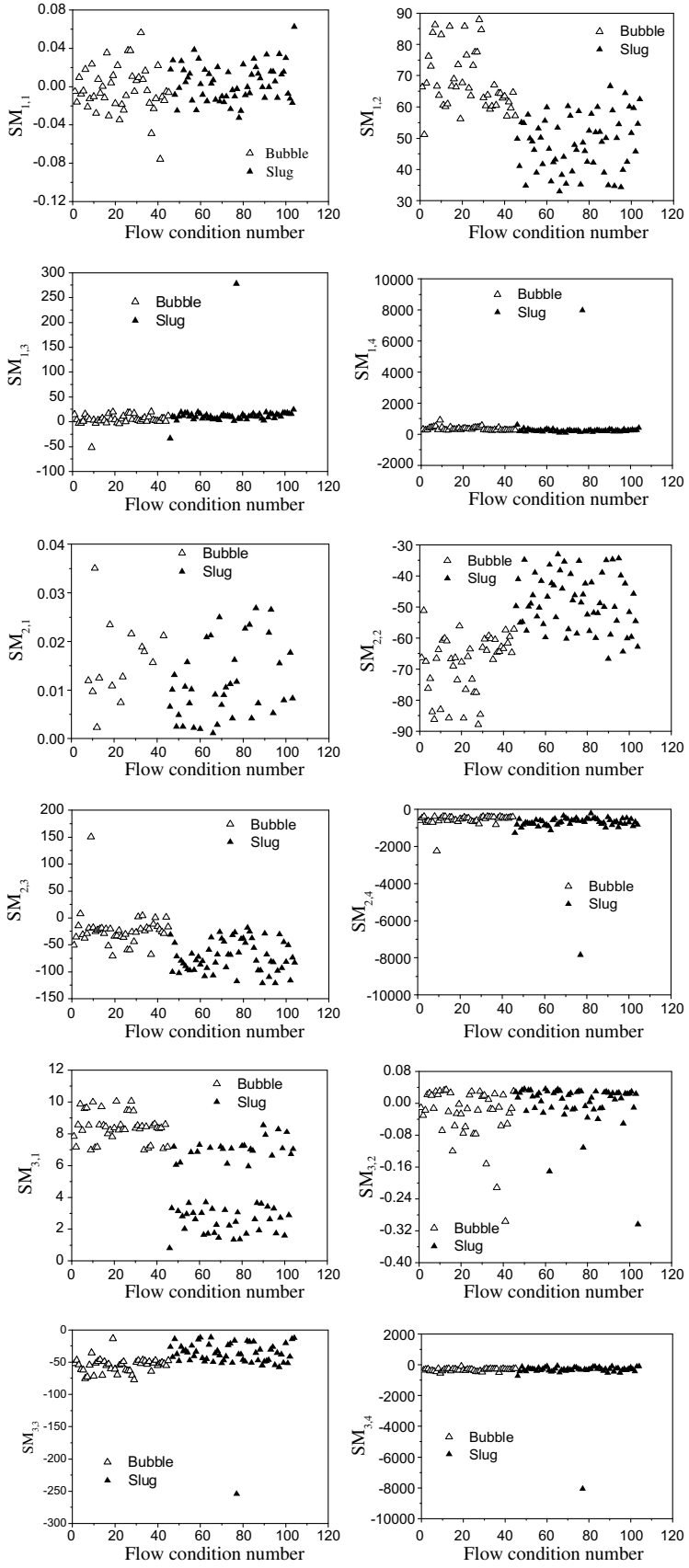

Fig. 12. Flow patterns distribution of 104 flow conditions on different attractor morphologic characteristic plot.

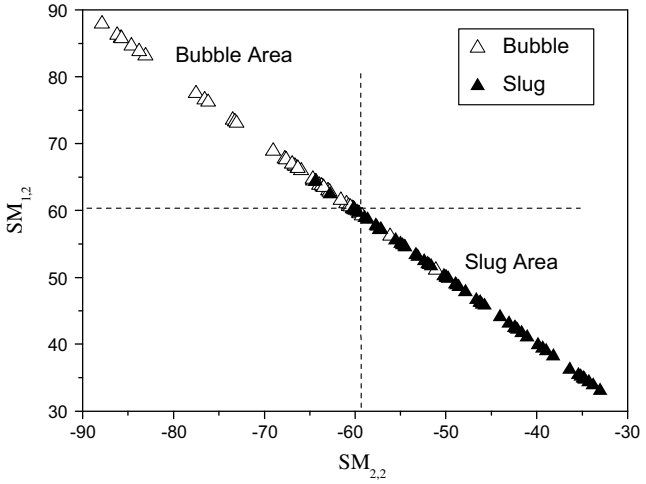

Fig. 13. Flow patterns distribution of different flow conditions on the $SM_{2,2} \sim SM_{1,2}$ plot.

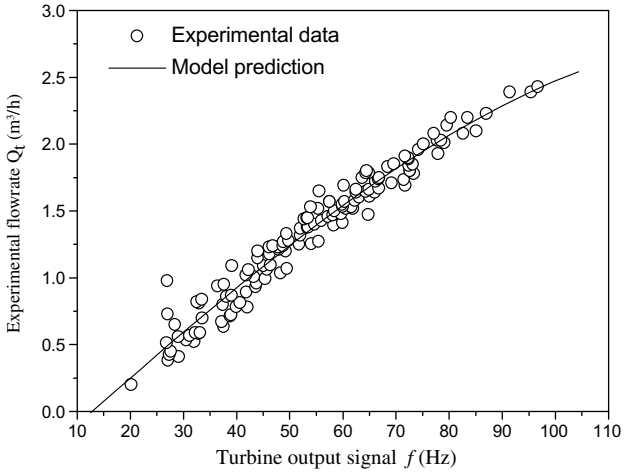

Fig. 14. Turbine flowmeter response in gas–water two phase flow.

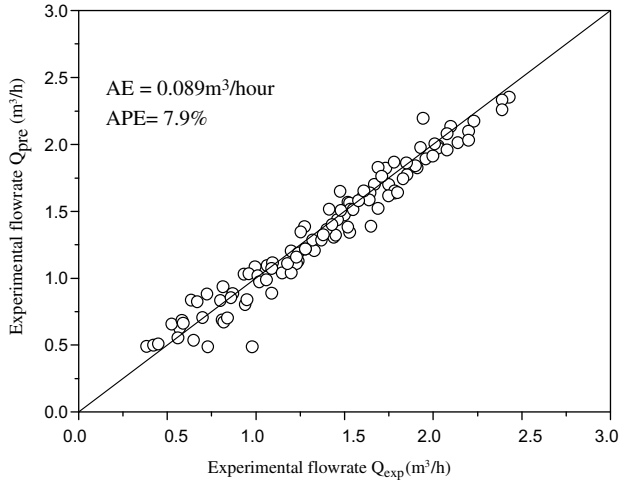

Fig. 15. Total flowrate prediction accuracy using the statistical model.

conductance signals in both time and frequency domains as the characteristic data set of SVM, which include maximum value (Max), the minimum value (Min), the average value ($\overline{Z}$), the standard deviation (SD), the asymmetric coefficient (CS) the kurtosis function (CK) in time domain, the four coefficients a_1, a_2, a_3, a_4 of a linear prediction model in frequency domain, and the average value of turbine rotate speed.

The maximum and minimum values could well reflect the conductivity of two phase flow, showing the fluctuant degree of the holdup of the non-conductible phase, which is in close relationship with the evolvement of the flow patterns; the average value reflects the average of fluctuant conductance signals; the standard deviation shows the discrete degree of the measured data; the asymmetric coefficient reflects the asymmetric degree of the sample comparing to the average value; the kurtosis function denotes the deviation of the sample distribution from the normal distribution. These feature extraction methods in time domain are all the basic methods in statistics, which are easy and quick. The definition of each characteristic is defined as followed, in which n is the number of data points, z_i is the ith data point.

The maximum (minimum) value is defined as

$$\begin{aligned} \mathrm{Max} &= \max(z_1, z_2, \ldots, z_n), \quad \mathrm{Min} \\ &= \min(z_1, z_2, \ldots, z_n) \end{aligned} \tag{14}$$

The average value of the all data is defined as

$$\overline{Z} = \frac{\sum_{i=1}^{n} z_i}{n-1} \tag{15}$$

The standard deviation is used to analyze the discrete degree of data, which is defined as

$$\mathrm{SD} = \left(\frac{\sum_{i=1}^{n} (z_i - \overline{Z})^2}{n-1} \right)^{1/2} \tag{16}$$

The asymmetric coefficient reflects the asymmetric degree of the sample around the average value, and could be defined as

$$\mathrm{CS} = \frac{\sum_{i=1}^{n} (z_i - \overline{Z})^3}{(n-1) \cdot \mathrm{SD}^2} \tag{17}$$

The kurtosis function is used to show the deviation degree of the sample distribution from the normal distribution, if the bending value is smaller than the standard value, it means the sample shows a platy kurtosis distribution; or if the bending value is larger than the standard value, it shows high kurtosis distribution. The kurtosis function is defined as

$$\mathrm{CK} = \left(\frac{\sum_{i=1}^{n} (z_i - \overline{Z})^4}{(n-1) \cdot \mathrm{SD}^4} \right) - 3 \tag{18}$$

The extraction of those frequency characteristics from the fluctuant signals of two phase flow refers to the linear prediction method in speech signal processing (Darwich et al., 1991; Makhoul, 1975), which has provided a simple and useful way to extract characteristics in frequency

domain. The linear prediction method is often used in analyzing and processing the speech signals, whose basic thinking is that: the current value of a signal could be estimated by the linear combination of values of several prior signals acquired; the linear coefficients could be worked out by making the variance (the energy of the error signals) between the estimated value and the true value of the signal minimum. These coefficients together compose a linear prediction model, and the number of the coefficients is called the order of this prediction model. We could study the smooth envelop of the speech frequency spectrum by using this linear prediction analysis method. Commonly speaking, the coefficients of the linear prediction model are just what we want to extract as the frequency characteristics from multiphase flow.

Assuming the output z_t of signals could be expressed as follow:

$$z_t = -\sum_{k=1}^{p} a_k z_{t-k} + G\sum_{l=0}^{q} b_l U_{t-l} \quad b_0 = 1 \tag{19}$$

where U_{t-l} is the unknown input signals, $a_k(1 \leqslant k \leqslant p)$, $b_l(1 \leqslant l \leqslant q)$ and G are all the system parameters, of which, G is the system gain, and $a_k(1 \leqslant k \leqslant p)$, the coefficients of the linear combination, are just what we want as the frequency characteristics. Eq. (19) shows that the output z_t is the linear function of current and former inputs, which is why this is called linear prediction.

As the input signal U_t is totally unknown, the input signal z_t could only be estimated from the former input approximately, which is

$$\widetilde{z}_t = -\sum_{k=1}^{p} a_k z_{t-k} \tag{20}$$

where $\widetilde{z}_t$ is the approximation of z_t, the deviation between them is

$$e_t = z_t - \widetilde{z}_t = z_t + \sum_{k=1}^{p} a_k z_{t-k} \tag{21}$$

The sum of squares of the deviation is

$$E = \sum_t e_t^2 = \sum_t \left(z_t + \sum_{k=1}^{p} a_k z_{t-k} \right)^2 \tag{22}$$

To determine a_k by the least square method, we have

$$\frac{\partial E}{\partial a_i} = 0 \quad 1 \leqslant i \leqslant p \tag{23}$$

That is

$$\sum_{k=1}^{p} a_k \sum_t z_{t-k} z_{t-i} = -\sum_t z_t z_{t-i}, \quad 1 \leqslant i \leqslant p \tag{24}$$

Eq. (24) shows that by giving fixed z_t, the coefficients $a_k(1 \leqslant k \leqslant p)$ can be worked out from this function group (including p functions and p unknown variables).

For different fluctuant signals, different characteristics can be gotten by this method, so that $a_k(1 \leqslant k \leqslant p)$ could be set as the characteristics of the fluctuant signals of the two phase flow. Usually, we choose the linear prediction model with four orders, so the characteristics are a_1, a_2, a_3, a_4.

6.2. The SVM model for water cut prediction

The SVM is usually used to solve the classification problems, but it could also be applied to the regression problems by simply introducing the loss function. There are linear regression and nonlinear regression in SVM, considering the nonlinear characteristics of the sample in this study, we chose the nonlinear regression model to improve the prediction precision.

Assuming the input sample x is an n-dimension vector, k samples and their corresponding output value y could be denoted as

$$(x_1, y_1), \ldots, (x_k, y_k), \quad x_k \in R^n, \quad y_k \in R \tag{25}$$

Firstly, we should find a linear fit function,

$$f(x) = \langle w \cdot x \rangle + b \tag{26}$$

where $\langle \cdot \rangle$ is the dot product of two vectors.

The best regression function could be gotten by working out the minimum solution of the function shown as follow:

$$\Phi(w, \xi) = \frac{1}{2}\|w^2\| + C\sum_{i=1}^{k}(\xi_i^- + \xi_i^+) \tag{27}$$

where C is the initialized penalty factor, used to control the penalty level to samples with errors outrun the appointed scope; ξ^+, ξ^- are the relax factors, showing the upper limit and lower limit of the sample errors.

We usually adopt the ε-insensitive loss function shown as Eq. (28), which means if the error of sample x is in the appointed tolerant scope ε, it is set to be ξ, without counting the loss when $|\xi| \leqslant \varepsilon$; or it is set to be $|\xi| - \varepsilon$.

$$L_\varepsilon(y) = \begin{cases} 0 & \text{for } |f(x) - y| < \varepsilon \\ |f(x) - y| - \varepsilon & \text{otherwise} \end{cases} \tag{28}$$

By constructing the Lagrange function, we could get dual equation shown as (29) of Eq. (27),

$$\begin{aligned} \max_{\alpha,\alpha^*} W(\alpha, \alpha^*) = {} & \max_{\alpha,\alpha^*} \sum_{i=1}^{k} \alpha_i^*(y_i - \varepsilon) - \alpha_i(y_i + \varepsilon) \\ & - \frac{1}{2}\sum_{i=1}^{k}\sum_{j=1}^{k}(\alpha_i^* - \alpha_i)(\alpha_j^* - \alpha_j)K(x_i, x_j) \\ \text{s.t.} \ & \sum_{i=1}^{k}(\alpha_i - \alpha_i^*) = 0, \quad \alpha_i, \alpha_i^* \in [0, C], \quad i = 1, \ldots, k \end{aligned} \tag{29}$$

where α and α^* are Lagrange multipliers, $K(x, x_i) = \varphi(x_i) \cdot \varphi(x_j)$ is called as the kernel function, $\varphi(x)$ is the mapping function from the sample space to the high-dimension characteristic space. The kernel function is expressed as the dot product of two $\varphi(x)$. By adopting the

kernel function, it is unnecessary to work out specifically the mapping function $\varphi(x)$, which makes the solving of nonlinear regression problems be possible.

Solving Eq. (29), the Lagrange multiplier α, α^* can be determined and the regression function is given by

$$f(x) = \sum_{i=1}^{k}(\alpha_i - \alpha_i^*)K(x_i, x) + b \tag{30}$$

where the sample x_i corresponding to weight value $(\alpha_i - \alpha_i^*)$ that is not zero is called the support vector. Obviously, the number of the support vectors determines the computational complexity. For the above SVM regression functions, when $|f(x_i) - y_i| \geqslant \varepsilon$, the weight value $(\alpha_i - \alpha_i^*)$ is not zero, then the corresponding sample x_i is the support vector.

The SVM is based on the structural risk minimization principle, not the traditional empirical risk minimization. It has considered both the fitness and complexity of the training sample, which means better generalization ability, but the parameters chosen for model will also largely influence the generalization ability of the model. In this study, we choose ε-insensitive function as the loss function of SVM, in which ε is set to 0.001, and we also choose Gaussian function as the kernel function:

$$K(x_i, x) = \exp(-\|x - x_i\|^2/\sigma^2) \tag{31}$$

The above equation could also be written as follow:

$$K(x_i, x) = \exp(-\gamma\|x - x_i\|^2) \tag{32}$$

By 5-folds cross-validation, we could get γ and C as the best parameters of the model.

6.3. The water cut prediction results

We have extracted 11 kinds of characteristics from 104 groups of conductance signals by using the above method, that is $\{f, \mathrm{Max}, \mathrm{Min}, \overline{Z}, \mathrm{SD}, \mathrm{CS}, \mathrm{CK}, a_1, a_2, a_3, a_4\}$, serves as the input vectors of SVM, symbolized by $\{x_1, x_2, x_3, x_4, x_5, x_6, x_7, x_8, x_9, x_{10}, x_{11}\}$. We have also divided the 104 groups of data in two parts, in which one part is used for training and the other are used for prediction. Setting up the precise prediction model is based on proper training data, if the training data is not chosen reasonably; there could not be satisfactory prediction result. In order to make the prediction result more accurate and reliable, training and predicting data should both cover the full range of the flowrate and water cut, basing on this principle, we chose 88 groups of data for training, and the remained 16 groups of data are used for predicting.

Fig. 16 shows the training result of 88 groups of data and Fig. 17 shows the prediction result of 16 groups of data under different flow conditions using the SVM, from the computational result we could know that the average error for water cut prediction is 0.038, which proves the model established by the SVM for volume fraction prediction could give us satisfactory result.

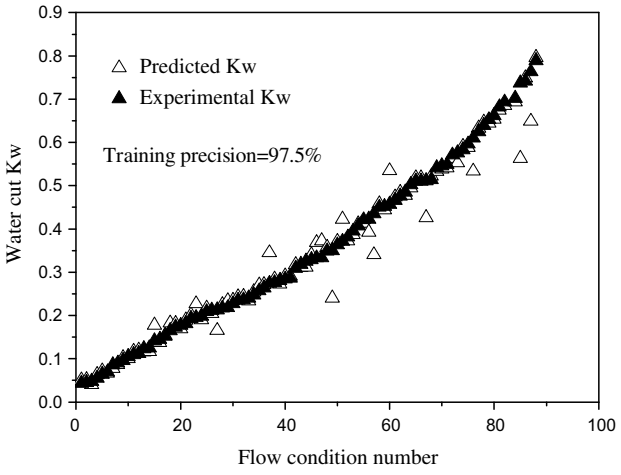

Fig. 16. SVM water cut model training results of 88 flow conditions.

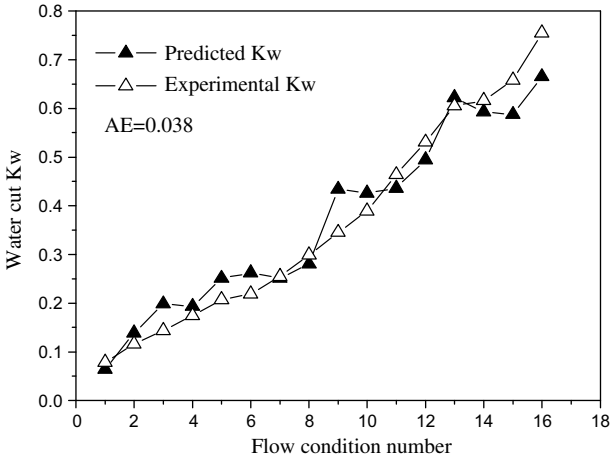

Fig. 17. Water cut prediction results of 16 flow conditions.

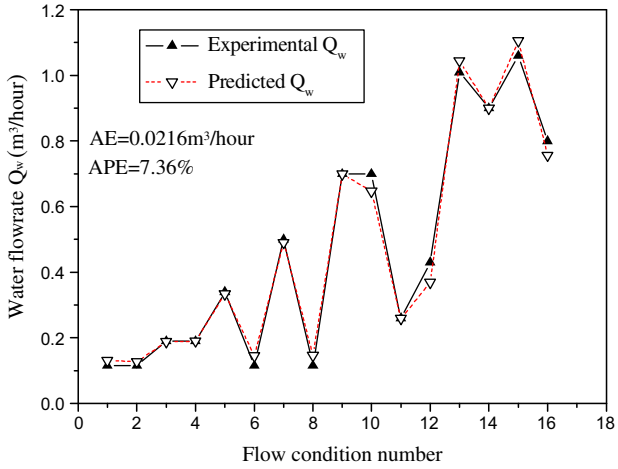

Fig. 18. Predicted result of water phase flowrate.

Figs. 18 and 19 are individual phase flowrate computed according to the predicted total flowrate and water cut,

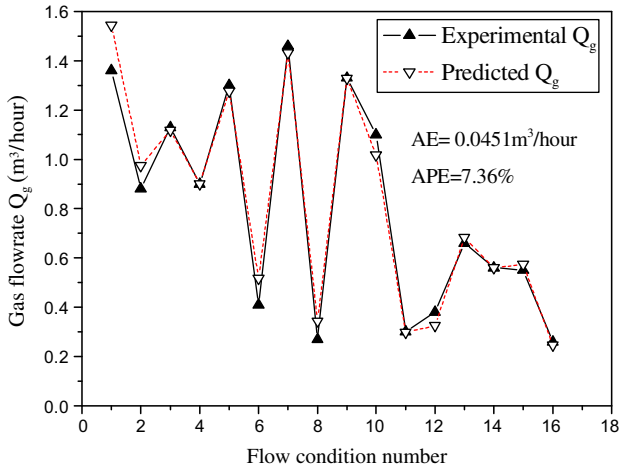

Fig. 19. Predicted result of gas phase flowrate.

respectively. Their average percent errors are 7.36%. The results of individual phase flowrate indicate it is a feasible way of measuring gas–liquid two phase flow using the combination of turbine flowmeter, conductance sensors and soft measurement method.

7. Conclusions

It is a new attempt to measure gas–liquid two phase flow flowrate employing combination instrument of turbine flowmeter and conductance sensor with petal type concentrating flow diverter and the results indicate that this method can realize the flowrate measurement of gas–liquid two phase flow with satisfactory precision. Although the original signals and their PDF, as well as PSD, can give some indications of flow patterns in the concentrating flow channel at some extent, the classification results tend to influenced by subjectivities, which are not suitable for quick and correct classification of flow patterns. The method of attractor morphologic characteristics synthetically represents the behaviors of attractors at different delay time, which can attenuate the influence of improper selected delay time. It has the feature of simple calculation and should be a good method to analyze the engineering nonlinear fluctuant signal. Because of the high accuracy and linear classifiable feature it has exhibited on flow pattern identification, the method can be used for reference to study complex flow conditions.

Adopted petal type concentrating flow method when measuring gas–liquid two phase flow, at some degree, the inhomogeneity of fluid in measurement channel is improved and the nonlinearity of performance of turbine and conductance sensors can be decreased. The characteristics extracted from conductance signals can reflect the change of volume fraction of flow conditions. The SVM soft measurement model can fulfill the quick and precise prediction of water cut based on the data set made up of conductance characteristics.

Acknowledgement

The study has been supported by National Nature Science Foundation of China (Grant Nos. 50674070 and 60374041).

References

Abdul-Razzak, A., Shoukri, M., Chang, J.S., 1995a. Measurement of two-phase refrigerant liquid–vapor mass flow rate – part II: turbine and void fraction meters. In: Proceedings of the 1995 ASHRAE Annual Meeting, CA, USA, pp. 523–531.

Abdul-Razzak, A., Shoukri, M., Chang, J.S., 1995b. Measurement of two-phase refrigerant liquid–vapor mass flow rate – part III: combined turbine and venturi meters and comparison with other methods. In: Proceedings of the 1995 ASHRAE Annual Meeting, CA, USA, pp. 532–538.

Annunziato, M., Abarbanel, H.D.I., 1999. Non linear dynamics for classification of multiphase flow regimes. In: Proceedings of International Conference on Soft Computing, Genova, Italy.

Darwich, T.D., Toral, H., Archer, J.S., 1991. A software technique for flow-rate measurement in horizontal two-phase flow. SPE Prod. Eng., 265–270.

Franca, F., Acikgoz, M., Lahey, R.T., Clausse, A., 1991. The use of fractal techniques for flow regime identification. Int. J. Multiphase Flow 17, 545–552.

Frank, R., Mazars, J., Ricque, R., 1977. Determination of Mass Flow Rate and Quality Using a Turbine Meter and a Venturi, Heat and Fluid Flow in Water React Safety, Conference. Mech. Eng. Publ. Ltd., Manchester, England, pp. 63–68.

Hardy, J.E., Hylton, J.O., 1984. Electrical impedance string probes for two-phase void and velocity measurements. Int. J. Multiphase Flow 10, 541–556.

Huang, Z., Xie, D., Zhang, H., Li, H., 2005. Gas–oil two-phase flow measurement using an electrical capacitance tomography system and a Venturi meter. Flow Meas. Instrum. 16, 177–182.

Jin, N.D., Zhang, J.X., Zhao, X., 2006. A study on soft measurement method of water holdup for gas/liquid two phase flow. In: The Sixth World Congress on Intelligent Control and Automation, 2006, Dalian, China, pp. 4890–4894.

Johnson, M.W., Farroll, S., 1995. Development of a turbine meter for two-phase flow measurement in vertical pipes. Flow Meas. Instrum. 6, 279–282.

Jones, O.C., 1983. Two-Phase Flow Measurement Techniques in Gas–Liquid Systems. Hemisphere Publishing, pp. 479–558.

Jones, O.C., Zuber, N., 1975. The interrelation between void fraction fluctuations and flow patterns in two-phase flow. Int. J. Multiphase Flow 2, 273–306.

Kelessidis, V.C., Dukler, A.E., 1989. Modeling flow pattern transitions for upward gas–liquid flow in vertical concentric and eccentric annuli. Int. J. Multiphase Flow 15, 173–191.

Lucas, G.P., Cory, J.C., Waterfall, R.C., 2000. A six-electrode local probe for measuring solids velocity and volume fraction profiles in solids-water flows. Meas. Sci. Technol. 11, 1498–1509.

Llauro, F.X., Llop, M.F., 2006. Characterization and classification of fluidization regimes by non-linear analysis of pressure fluctuations. Int. J. Multiphase Flow 32, 1397–1404.

Ma, Y.P., Bei, B.S., Lin, W.K., Yih-Chyun, T., Yih-Yun, H., 1990. An impedance method to determine void fraction for two-phase flow. Nucl. Sci. J. 27, 315–326.

Makhoul, J., 1975. Linear prediction: a tutorial review. Proc. IEEE 63, 561–580.

Mark, P.A., Johnson, M.W., Sproston, J.L., Millington, B.C., 1990. The turbine meter applied to void fraction determination in two-phase flow. Flow Meas. Instrum. 1, 246–252.

Matsui, G., 1984. Identification of flow regimes in vertical gas–liquid two-phase flow using differential pressure fluctuations. Int. J. Multiphase Flow 10, 711–719.

Mendes, M.L., Marvillet, C., 1996. Local measurements in gas–liquid two-phase flows: a review of different techniques. In: Proceedings of the 1996 ASME Fluids Engineering Division Summer Meeting. Part 4 (of 4). American Society of Mechanical Engineers, Fluids Engineering Division (Publication) FED, CA, USA, pp. 363–370.

Minemura, K., Egashira, K., Ihara, K., Furuta, H., Yamamoto, K., 1996. Simultaneous measuring method for both volumetric flow rates of air–water mixture using a turbine flowmeter. J. Energy Resour. Technol. Trans. ASME 118, 29–35.

Oddie, G., Pearson, J.R., 2004. Flow-rate measurement in two-phase flow. Ann. Rev. Fluid Mech. 36, 149–172.

Ogawa, Y., Kawaoto, H., Gu, R.L., Yamashita, M., Shoda, S., 1998. Experiments of a turbine meter for multiphase flow. In: Proceedings of 9th International Conference on Flow Measurement, Lund, Sweden, pp. 285–290.

Peng, Z.R., Mi, G.S., 2006. Voidage measurement of two-phase flow based on least squares support vector machine. In: The Sixth World Congress on Intelligent Control and Automation, 2006, Dalian, China, pp. 4900–4903.

Peng, Z.R., Liu, S.Z., 2006. Concentration measurement of two-phase flow by means of LS–SVM. In: International Conference on Machine Learning and Cybernetics, 2006, pp. 3667–3670.

Shim, W.J., Lee, C.T., 1998. Measurement of gas–liquid vertical upward flow using turbine flow meter. In: Proceedings of the 1998 ASME/JSME Pressure Vessels and Piping Conference, CA, USA, pp. 171–176.

Shim, W.J., Dougherty, T.J., Cheh, H.Y., 1996. Turbine flow meter response in two-phase flows. In: Proceedings of the 1996 4th ASME/JSME International Conference on Nuclear Engineering, New Orleans, USA, pp. 943–954.

Takens, F., 1981. Dynamical system and turbulence. Lecture Note in Mathematics, p. 336.

Vapnik, V.N., 1995. The Nature of Statistical Learning Theory. Springer, New York.

Vapnik, V.N., 1999. An overview of statistical learning theory. IEEE Trans. Neural Netw. 10, 988–999.

Vince, M.A., Lahey, R.T., 1982. On the development of an objective flow regime indicator. Int. J. Multiphase Flow 8, 93–124.

Xiao, N., Jin, N.D., 2007. Research on flow pattern classification method of two phase flow based on chaotic attractor morphological characteristic. Acta Phys. Sin. 56, 5149–5157.

Yang, H.C., Kim, D.K., Kim, M.H., 2003. Void fraction measurement using impedance method. Flow Meas. Instrum. 14, 151–160.